J. Am. Chem. Soc. **1986**, *108*, 4368–4378

Gas-Phase Nucleophilic Addition Reactions of Negative Ions with Transition-Metal Carbonyls

Kelley R. Lane, Larry Sallans, and Robert R. Squires*

Contribution from the Department of Chemistry, Purdue University, West Lafayette, Indiana 47907. *Received November 13, 1985*

Abstract: Gas-phase ion–molecule reactions between $Fe(CO)_5$ and an extensive series of negative ions have been investigated with a flowing afterglow apparatus operating at 300 K. Reaction generally proceeds by nucleophilic addition of an anion (X^-) to produce $(CO)_4FeC(O)X^-$, $(CO)_4FeX^-$, and $(CO)_3FeX^-$ products by displacement of zero, one, and two CO ligands, respectively. Other products derived from atom-, ion-, or electron-transfer reactions are also observed in some cases. In general, strongly basic, localized, heteroatomic anions produce metal ion products exhibiting a greater extent of CO loss than do weakly basic, delocalized ions and carbanions. Pressure-dependent product distributions are evident for certain of the reactions wherein the observed extent of CO loss from the products smoothly decreases with increasing pressure in the flow reactor. A unified mechanism for gas-phase negative ion condensation reactions of $Fe(CO)_5$ is postulated based on the observed product ratios, measured kinetics, and estimated thermochemistry: Initial addition of a nucleophilic anion to a CO ligand produces an energy-rich iron–acyl complex that subsequently undergoes sequential dissociation of up to two carbonyls in competition with collisional stabilization of the fragmenting intermediates. Dissociation of the first CO from the acyl complex is followed by migratory deinsertion of the nucleophile to form an excited $(CO)_4FeX^-$ complex. Loss of the second CO may then occur in competition with collisional deactivation. A kinetic model is formulated based on the proposed mechanism and the observed pressure dependence which allows estimates to be made of the CO dissociation lifetimes for several of the postulated intermediates. Estimates of relevant bond energies for the metal ion intermediates are also described which permit the construction of a semiquantitative energy profile for each negative ion reaction.

Nucleophilic substitution and addition reactions represent a cornerstone of chemical research. Physical organic chemistry owes its very origins to the study of nucleophilic reactions,[1,2] and these processes have traditionally played a central role in our understanding of kinetics, reaction dynamics, stereochemistry, and substituent effects.[3] Substitution and addition reactions of nucleophiles are pervasive in both organic and organometallic synthesis, with modern refinements providing a potent arsenal of tools for complex molecule construction.[4] Nucleophilic addition reactions are particularly conspicuous in organometallic chemistry pertaining to small-molecule activation via homogeneous catalysis. For example, base-catalyzed nucleophilic additions to metal carbonyls and related coordination compounds lie at the heart of industrially important catalytic cycles such as the water-gas shift, Fischer–Tropsch, Reppe, and Wacker–Schmidt processes.[5] More recent attempts to activate CO_2 in homogeneous solution have commonly involved transition-metal mediated C/C or C/H bond formation under nucleophilic conditions.[6,7] For more complex (stoichiometric) carbon–carbon bond-forming reactions, Fischer[8] and others[9,10] have shown that nucleophilic addition of organoalkali reagents to simple metal carbonyls and other organometallic complexes affords versatile intermediates for selective organic syntheses.

Accordingly, considerable effort has been dedicated over the years to the study of the scope and mechanisms of nucleophilic reactions involving organometallic complexes.[5] Mononuclear metal carbonyls such as $Fe(CO)_5$ and the group 6 hexacarbonyls are frequently employed as model compounds for these studies and the general features of their reactivity are well-documented.[11–13] Recognizing the profound impact that gas-phase ion studies have made on our understanding of nucleophilic displacement and addition reactions of *organic* compounds,[14,15] we felt that an analogous examination of nucleophilic addition reactions involving transition-metal carbonyls was warranted in order to differentiate intrinsic effects and medium effects on their reactivity. In this paper we describe in detail the gas-phase reactions of $Fe(CO)_5$ with an extensive series of negative ions as characterized by the flowing afterglow technique. Kinetic measurements, product distributions, and thermochemical data for these reactions are presented, along with a unified reaction profile derived from the observed trends.

Previous investigations of the reactions between negative ions and volatile metal carbonyls have been carried out almost exclusively at low pressure ($<10^{-6}$ torr) using ion cyclotron resonance (ICR).[16–18] In one of the earliest studies involving $Fe(CO)_5$, Beauchamp and Foster reported that the relatively basic anions[19] F^- and $CH_3CH_2O^-$ reacted to produce a single ionic product arising from addition followed by loss of two CO ligands (eq 1).[16]

(1) Hughes, E. D.; Ingold, C. K.; Patel, J. *J. Chem. Soc.* **1933**, 526. (b) Gleave, J. L.; Hughes, E. D.; Ingold, C. K. *J. Chem. Soc.* **1935**, 236. (c) Hughes, E. D.; Ingold, C. K. *J. Chem. Soc.* **1935**, 244.

(2) Kenyon, J.; Phillips, H.; Turley, H. G. *J. Chem. Soc.* **1925**, 399.

(3) For comprehensive texts, see: (a) Hammet, L. P. *Physical Organic Chemistry, Reaction Rates, Equilibria and Mechanisms*; McGraw-Hill: New York, 1940; (b) Hine, J. *Physical Organic Chemistry*; McGraw-Hill: New York, 1956; (c) Wiberg, K. B. *Physical Organic Chemistry*; Wiley: New York, 1964; (d) Ritchie, C. D. *Physical Organic Chemistry, The Fundamental Concepts*; Marcel Dekker: New York, 1975.

(4) (a) House, H. O. *Modern Synthetic Reactions*; W. A. Benjamin: Menlo Park, CA, 1972. (b) Wilkinson, G., Ed. *Comprehensive Organometallic Chemistry*; Pergamon: New York, 1982.

(5) (a) Cotton, F. A.; Wilkinson, G. *Advanced Inorganic Chemistry; A Comprehensive Text*; Wiley: New York, 1980. (b) Collman, J. P.; Hegedus, L. S. In *Principles and Applications of Organotransition Metal Chemistry*; Kelley, A., Ed.; University Science: Mill Valley, CA, 1980.

(6) Darensbourg, D. J.; Kudaraski, R. A. *Adv. Organomet. Chem.* **1984**, *106*, 3905 and references therein.

(7) Gladysz, J. A. *Adv. Organomet. Chem.* **1982**, *20*, 1 and references therein.

(8) Fischer, E. O.; Maasbol, A. *Angew. Chem., Int. Ed. Engl.* **1964**, *3*, 580.

(9) Collman, J. P. *Acc. Chem. Res.* **1975**, *8*, 342 and references therein.

(10) Semmelhack, M. F.; Clark, G. R.; Garcia, J. L.; Harrison, J. J.; Thebtaranonth, Y.; Wulf, W.; Yamashita, A. *Tetrahedron*, **1981**, *23*, 3957 and references therein.

(11) (a) Darensbourg, D. J.; Rokicki, A. *Organometallics* **1982**, *1*, 1685. (b) Dobson, G. R. *Acc. Chem. Res.* **1976**, *9*, 300. (c) Darsenbourg, M. Y.; Darensbourg, D. J. *Inorg. Chem.* **1970**, *9*, 32.

(12) Pettit, R.; Cann, K.; Cole, T.; Maneden, C.; Slegeir, W. *Adv. Chem. Ser.* **1979**, *No. 173*, 121–130.

(13) Trautmann, R. J.; Gross, D. C.; Ford, P. C. *J. Am. Chem. Soc.* **1985**, *107*, 2355.

(14) (a) Olmstead, W. N.; Brauman, J. I. *J. Am. Chem. Soc.* **1977**, *99*, 4219. (b) Asubiojo, O. I.; Brauman, J. I. *J. Am. Chem. Soc.* **1979**, *101*, 3715. (c) Pellerite; M. J.; Brauman, J. I. *J. Am. Chem. Soc.* **1980**, *102*, 5993.

(15) Caldwell, G.; Magnera, T. F.; Kebarle, P. *J. Am. Chem. Soc.* **1984**, *106*, 959.

(16) Foster, M. S.; Beauchamp, J. L. *J. Am. Chem. Soc.* **1975**, *97*, 4808.

(17) Corderman, R. R.; Beauchamp, J. L. *Inorg. Chem.* **1977**, *16*, 3135.

(18) Dunbar, R. C.; Ennever, J. F.; Fackler, J. P., Jr. *Inorg. Chem.* **1973**, *12*, 2734.

(19) (a) Bartmess, J. E.; McIver, R. T., Jr., In *Gas Phase Ion Chemistry*; Bowers, M. T., Ed.; Academic Press: New York, 1979; Vol. 2, Chapter 11. (b) Moylan, C. R.; Brauman, J. I. *J. Phys. Chem.* **1984**, *88*, 3175.

0002-7863/86/1508-4368$01.50/0

$$X^- + Fe(CO)_5 \rightarrow (CO)_3FeX^- + 2CO \quad (1)$$

$$X = F^-, CH_3CH_2O^-$$

The weaker base anions CN^- and Cl^- were observed to be unreactive. An analogous outcome was subsequently reported for $C_5H_5Co(CO)_2$[17] and the apparent correlation between anion basicity and reactivity was noted. In the present work we considerably expand and qualify this concept and describe the enhanced reactivity of $Fe(CO)_5$ with negative ions under flowing afterglow conditions (ca. 0.5 torr), where termolecular reactions become significant.

Experimental Section

All experiments were carried out at 300 ± 2 K in a flowing afterglow apparatus which we have described previously.[20] The system consists of a microprocessor-controlled quadrupole mass spectrometer with a 100 cm × 7.6 cm i.d. stainless steel flow reactor interposed between an electron-impact ion source and the ion-sampling orifice located in front of the quadrupole. Helium buffer gas flows through the reactor at a relatively high velocity (~90 m s^{-1}), flow rate (~180 STP cm^3 s^{-1}), and pressure (0.1–1.0 torr) as determined by a mass-flow controller and high-capacity Roots blower. Primary reactant ions generated in the ion-source region are rapidly thermalized by collisions with the helium buffer gas. Further downstream, the ions undergo reactions with gaseous reagents introduced into the reactor either through metering valves fixed at various positions along the length of the tube or via a moveable neutral injector. The moveable injector permits convenient determination of ion–molecule reaction rate coefficients under pseudo-first-order conditions by monitoring the decay of a reactant ion signal as a function of injector position (reaction time). Neutral reagent flow rates are measured by momentarily diverting the flow to a calibrated volume and monitoring the pressure increase with time. In certain of the kinetics measurements in this study we encountered significant curvature in the reactant ion decay plots at long reaction times (distances). We attributed this to facile dissociative attachment of free electrons by $Fe(CO)_5$ when it entered the reactor at positions near the ion-source region.[21] The excessively large buildup of $Fe(CO)_4^-$ (m/z 168) that resulted evidently produced significant perturbations on the observed intensities of other ions in the system, presumably through changes in the ion diffusion characteristics in the flowing plasma or through interference with ion sampling at the nosecone. This problem could be minimized by adding sufficient SF_6 to the system just after the ion-source region (ca. 0.05 STP cm^3 s^{-1}) to act as an electron scavenger. Under these conditions the undesirable buildup of $Fe(CO)_4^-$ was attenuated and linear kinetic plots could be obtained for all negative ions examined. Rate coefficients were routinely measured with a precision better than ±1% and estimated accuracies of ±20%. Primary product distributions for ion–molecule reactions were determined by documented procedures[22,23] and are estimated to be reliable to better than ±10%.

Most all primary reactant ions were generated via proton abstraction from the corresponding neutral acid by NH_2^- or OH^-, the former being produced by electron impact on NH_3 and the latter from electron impact on a 2:1 mixture of CH_4 and N_2O. Hydride ion was generated by electron impact on low flow rates of NH_3 in the presence of excess H_2. The alkoxides and the carboxylate ions were produced either by proton transfer or by direct electron impact with the neutral conjugate acids. Fluoride and chloride ions were produced by electron impact on the corresponding tetrahalomethanes, and Br^- and I^- were generated from electron ionization of the ethyl- and methylhalides, respectively. Azide ion was generated from the rapid reaction between NH_2^- and N_2O.[24]

All reagent gases were obtained from commercial suppliers and were of the following purities: He, 99.995%; NH_3, 99.99%; N_2O, 99.0%; CH_4, 99.0%; CH_2=$CHCH_3$, 99.0%; C_2H_2, 99.6%; H_2S, 99.5%; H_2, 99.0%; CO_2, 99.5%; SF_6, 99.8%. Liquid samples were also obtained commercially and used as supplied except for occasional addition of $LiAlH_4$ when permissible to ensure reagent dryness, as well as multiple freeze–pump–thaw cycles to remove noncondensible impurities.

(20) Lane, K. R.; Lee, R. E.; Sallans, L.; Squires, R. R. *J. Am. Chem. Soc.* **1984**, *106*, 5767.
(21) George, P. M.; Beauchamp, J. L. *J. Chem. Phys.* **1982**, *76*, 2959.
(22) (a) Smith, D.; Adams, N. G. In *Gas Phase Ion Chemistry*; Bowers, M. T., Ed.; Academic Press: New York, 1979; Vol. 1 Chapter 1. (b) Adams, N. G.; Smith, D. *J. Phys. B.* **1976**, *9*, 1439.
(23) (a) Anderson, D. R.; Bierbaum, V. M.; DePuy, C. H. *J. Am. Chem. Soc.* **1983**, *105*, 4244. (b) Anderson, D. R.; Bierbaum, V. M.; DePuy, C. H.; Grabowski, J. J. *Int. J. Mass Spectrum. Ion Proc.* **1983**, *52*, 65.
(24) Bierbaum, V. M.; Depuy, C. H.; Shapiro, R. H. *J. Am. Chem. Soc.* **1977**, *99*, 5800.

Table I. Reactions of NH_2^-, H^-, and HO^- with $Fe(CO)_5$ at 0.4 torr

anion	PA[a]	k^{11}[b]	eff	primary product ions (%)	secondary product ions
NH_2^-	403.6	2.3	0.72	$(CO)_3FeNH_2^-$ (100)	$H_2NFe_2(CO)_6^-$ $H_2NFe_2(CO)_7^-$
H^-	400.4	4.9	0.40	$(CO)_3FeH^-$ (64) $(CO)_4FeH^-$ (36)	$HFe_2(CO)_6^-$ $HFe_2(CO)_7^-$
OH^-	390.7	2.1	0.69	$(CO)_3FeOH^-$ (100)	$HOFe_2(CO)_6^-$ $HOFe_2(CO)_7^-$ $HOFe_2(CO)_8^-$

[a] Proton affinity in units of kcal mol^{-1}, ref 19. [b] In units of 10^{-9} cm^3 $molecule^{-1}$ s^{-1}.

Results

In the course of our survey of the reactions of $Fe(CO)_5$ with negative ions, we have examined over two dozen different reactant anions representing a broad variety of constitutions, basicities and structures. In contrast to the earlier ICR study,[16] we find that under the higher pressure conditions of the flowing afterglow, almost every anion we have examined reacts with $Fe(CO)_5$. The general reaction for most all negative ions is summarized in eq 2, where nucleophilic addition may be accompanied by loss of zero,

$$\begin{aligned} X^- + Fe(CO)_5 &\rightarrow (CO)_3FeX^- + 2CO \\ &\rightarrow (CO)_4FeX^- + CO \\ &\rightarrow (CO)_4FeC(O)X^- \end{aligned} \quad (2)$$

one, or two carbon monoxide ligands from the product ion complex. In several cases, interesting side reactions are also observed. In the following sections we present a systematic account of the rates and product distributions for the observed reactions, subdividing the reactant anions into nine different constitutional classes.

Hydride, Amide, and Hydroxide. We have previously described the gas-phase reactions of $Fe(CO)_5$ with OH^-[20] and H^-.[25] We repeat these data here along with the new results for NH_2^- as a collective class of strongly basic anion reactants. The primary product distributions, secondary products, bimolecular rate constants, and reaction efficiencies (eff = $k_{obsd}/k_{Langevin}$)[26] for each ion are presented in Table I. All ions react quite rapidly with rates near the ion–molecule collision limit. Both OH^- and NH_2^- produce exclusively an iron tricarbonyl product ion from expulsion of two CO ligands, while H^- induces loss of one and two CO ligands. Each of the 16-electron tricarbonyl product ions undergoes subsequent reactions with $Fe(CO)_5$ to yield dinuclear ion complexes from which zero, one, or two CO ligands are expelled. The 18-electron product ion $HFe(CO)_4^-$ does not react further with $Fe(CO)_5$ within the time scale available to our experiment. No change in the measured rates for any of these reactions is apparent over a range of helium pressure from 0.3 to 0.8 torr. While only tricarbonyl primary product complexes are observed from the NH_2^- and OH^- reactions over this pressure range, the primary $HFe(CO)_4^-/HFe(CO)_3^-$ branching ratio exhibits a slight pressure dependence, with the tricarbonyl product giving way to the tetracarbonyl ion as pressure is increased (vide infra).

Alkoxides. Alkoxide ions, generated by proton abstraction from the parent alcohol, generally produce only the tricarbonyl product ions $(CO)_3FeOR^-$. In some cases the iron tetracarbonyl formyl anion, $(CO)_4FeCHO^-$, is also produced by hydride-transfer reactions which we have documented previously[25] (eq 3). An adduct

$$R_2CHO^- + Fe(CO)_5 \rightarrow R_2CO + (CO)_4FeCHO^- \quad (3)$$

complex, believed to be the metalloester, $(CO)_4FeCO_2R^-$, is also observed in most every case. However, due to the unavoidable presence of the reactive alkoxide cluster ions $RO(ROH)_n^-$ or $RO(H_2O)^-$ in these experiments, we cannot unambiguously assign its origins to the unsolvated ion reactant. While accurate product branching ratio measurements are therefore precluded, we can assign the observed $(CO)_3FeOR^-$ products exclusively to the bare

(25) Lane, K. R.; Sallans, L.; Squires, R. R. *Organometallics* **1985**, *3*, 408.
(26) Su, T.; Bowers, M. T. In *Gas Phase Ion Chemistry*; Bowers, M. T., Ed.; Academic Press: New York, 1979; Vol. 1, Chapter 3.

Table II. Reactions of Alkoxide Ions with $Fe(CO)_5$ at 0.4 torr

alkoxide (RO^-)	PA[a]	k^{11}[b]	eff	primary product ions	secondary ions
CH_3O^-	381.4	1.8	0.76	$(CO)_3FeOR^-$	$ROFe_2(CO)_6^-$
				$(CO)_4FeCHO^-$	$ROFe_2(CO)_7^-$
					$ROFe_2(CO)_8^-$
$CH_3CH_2O^-$	376.1	1.4	0.69	$(CO)_3FeOR^-$	$ROFe_2(CO)_6^-$
				$(CO)_4FeCHO^-$	$ROFe_2(CO)_7^-$
					$ROFe_2(CO)_8^-$
$(CH_3)_3CO^-$	373.3	1.6	0.95	$(CO)_3FeOR^-$	
$MeOCH_2CH_2O^-$	372.5	1.9	1.1	$(CO)_3FeOR^-$	
				$(CO)_4FeCO_2R^-$	
				$(CO)_4FeCHO^-$	
$EtC(CH_3)_2O^-$	371.9[c]	1.0	0.63	$(CO)_3FeOR^-$	
				$(CO)_4FeCO_2R^-$	
n-$BuCH(CH_3)O^-$	371[d]	1.4	0.93	$(CO)_4FeCO_2R^-$	
				$(CO)_4FeCHO^-$	
$CF_3CH_2O^-$	364.4	1.3	0.86	$(CO)_3FeOR^-$	

[a] Proton affinity in units of kcal mol^{-1}, ref 19. [b] In units of 10^{-9} cm^3 $molecule^{-1}$ s^{-1}. [c] Boand, G.; Houriet, R.; Gaumann, T. *J. Am. Chem. Soc.* **1983**, *105*, 2203. [d] Estimated from data in *c*.

alkoxide reactants since they disappear completely when higher concentrations of the parent alcohol are added to the system and only the corresponding $RO(ROH)_n^-$ clusters are present. The results for eight alkoxides of varying size and substitution are summarized in Table II, listed in order of decreasing proton affinity.[19] All reactions are highly efficient. Hydride transfer is observed from each of the primary and secondary alkoxides except $CF_3CH_2O^-$.[25] The largest alkoxide, n-$BuCH(CH_3)O^-$, does not produce any observable tricarbonyl product and only the adduct ion $(CO)_4FeCO_2R^-$ is observed. While $RO(ROH)_n^-$ clusters are also present in this particular experiment, we believe the adduct to be a primary product from the bare ion since the alkoxide reacts away rapidly and completely in the presence of $Fe(CO)_5$. The $(CO)_3FeOR^-$ ions formed from CH_3O^- and $CH_3CH_2O^-$ are observed to undergo secondary condensation reactions with $Fe(CO)_5$ to produce dinuclear products $ROFe_2(CO)_n^-$, n = 6–8. No such secondary condensations can be observed with any of the other primary product ions due to their low primary yields. Variation of the helium pressure in the flow reactor over the range 0.3–0.8 torr does not produce any significant change in the measured rates of reaction nor appearance of new primary ionic products.

Thiolates. The thiolate ions HS^- and $CH_3CH_2S^-$ react with $Fe(CO)_5$ exclusively by termolecular addition (eq 4). The apparent bimolecular rates for these reactions at 0.4 torr are 7.8×10^{-10} and 1.2×10^{-9} cm^3 s^{-1} for HS^- and $CH_3CH_2S^-$, corresponding

$$RS^- + Fe(CO)_5 \xrightarrow{He} (CO)_4FeC(O)SR^- \qquad (4)$$

to efficiencies of 0.34 and 0.67, respectively. No significant change in either apparent bimolecular rate is observed when the reactor pressure is varied from 0.3 to 0.7 torr, indicating that the termolecular association reactions are saturated in this pressure range.[27] The adducts do not undergo any observable secondary reactions with $Fe(CO)_5$.

Enolates. The enolate ions derived by proton abstraction from acetone and 2-butanone react with $Fe(CO)_5$ by exclusive addition. The apparent bimolecular rate coefficients and corresponding efficiencies for these reactions at 0.4 torr are 1.3×10^{-9} (0.68) and 1.1×10^{-9} cm^3 s^{-1} (0.61) for $CH_3COCH_2^-$ and $CH_3COCH\text{-}CH_3^-$, respectively. As with the thiolates, no pressure dependence in the kinetics from 0.3 to 0.7 torr is observed, and the adducts are inert toward further reaction with $Fe(CO)_5$. We have previously presented arguments in support of the view that the observed negative ion adducts of $Fe(CO)_5$ are covalently bonded iron tetracarbonyl–acyl ions of the general structure $(CO)_4FeC(O)X^-$, as opposed to electrostatically bound cluster ions.[28] In the present case, the ambident nature of enolate ions creates uncertainty as to whether the observed adducts are bonded through carbon or oxygen. As will be shown later, the site of attachment may have an important influence on the outcome of reaction. Ellison and co-workers have recently demonstrated exclusive kinetic O-alkylation in gas-phase S_N2 reactions between methyl halides and cyclohexanone enolate.[29] However, whether this selectivity would also hold when $Fe(CO)_5$ is the electrophile is not immediately obvious.

Table III. Reactions of Carboxylate Ions with $Fe(CO)_5$ at 0.4 torr

carboxylate	PA[a]	k^{11}[b]	eff	primary product ions (%)
HCO_2^-	345.2	0.16	0.08	$(CO)_4FeC(O)O_2CH^-$ (75)
				$(CO)_4FeH^-$ (12)
				$(CO)_4FeCHO^-$ (13)
$CH_3CO_2^-$	348.5	0.14	0.08	$(CO)_4FeC(O)O_2CCH_3^-$ (100)
$CH_3OCO_2^-$		0.07	0.04	$(CO)_4FeCO_2CH_3^-$ (100)

[a] Proton affinity in units of kcal mol^{-1}, ref 19. [b] In units of 10^{-9} cm^{-3} $molecule^{-1}$ s^{-1}.

Table IV. Reactions of Carbanions with $Fe(CO)_5$ at 0.4 torr

carbanion (R^-)	PA[a]	k^{11}[b]	eff	primary product ions (%)
$C_6H_5^-$	398.8	1.4	0.84	$(CO)_3FeC_6H_5^-$ (40)
				$(CO)_4FeC_6H_5^-$ (60)
$CH_2{=}CHCH_2^-$	391.3	1.1	0.52	$(CO)_4FeR^-$ (11)
				$(CO)_4FeC(O)R^-$ (25)
				$(CO)_4Fe^-$ (64)
$C_6H_5CH_2^-$	379.4	1.3	0.83	$(CO)_3FeR^-$ (5)
				$(CO)_4FeR^-$ (5)
				$(CO)_4FeC(O)R^-$ (90)
$C_6H_5CHCH_3^-$	378.3	1.1	0.74	$(CO)_4FeR^-$ (10)
				$(CO)_4FeC(O)R^-$ (77)
				$(CO)_4FeH^-$ (10)
				$(CO)_4FeCHO^-$ (3)
HC_2^-	375.4	2.5	0.96	$(CO)_3FeR^-$ *c*
				$(CO)_4FeR^-$
				$(CO)_4FeC(O)R^-$
c-$C_6H_7^-$	370[d]	1.1	0.67	$(CO)_4FeC(O)R^-$ (16)
				$(CO)_4FeCHO^-$ (8)
				$(CO)_4FeH^-$ (12)
				$(CO)_4Fe^-$ (64)

[a] Proton affinity in units of kcal mol^{-1}, ref 19. [b] In units of 10^{-9} cm^3 $molecule^{-1}$ s^{-1}. [c] Branching ratio indeterminable; see text. [d] Kindy, M.; Lane, K. R.; Lee, R. E.; Squires, R. R., unpublished results.

Carboxylates. The reactions of three representative carboxylate ions with $Fe(CO)_5$ have been examined and a summary of results is provided in Table III. The carboxylates undergo somewhat slower reactions, with measured efficiencies about a factor of 10 less than all other reactive ions. Acetate ion reacts by termolecular addition to produce a mixed-anhydride product ion complex. The apparent rate does not increase up to 0.8-torr reactor pressure. Generation of acetate ion from acetic acid also necessarily produces hydrogen-bonded cluster ions $CH_3CO_2(CH_3CO_2H)_n^-$, n = 1–3, under our conditions; however, these ions are inert toward $Fe(CO)_5$. Formate ion can be conveniently produced in the absence of formic acid by taking advantage of the hydride-transfer reaction that occurs between CH_3O^- and carbon dioxide (eq 5).[30,31]

$$CH_3O^- + CO_2 \rightarrow HCO_2^- + CH_2O$$
$$\xrightarrow{He} CH_3OCO_2^- \qquad (5)$$

Methyl carbonate anion is also produced, so its reaction with $Fe(CO)_5$ was also characterized. Formate reacts to produce three primary products by direct addition, hydride transfer, and hydride transfer followed by loss of one CO ligand.[25] No secondary

(27) Bohme, D. K.; Dunkin, D. B.; Fehsenfeld, F. C.; Ferguson, *J. Chem. Phys.* **1969**, *51*, 863.
(28) Lane, K. R.; Sallans, L.; Squires, R. R. *J. Am. Chem. Soc.* **1985**, *107*, 5369.
(29) Jones, M. E.; Kass, S. R.; Filley, J.; Barkley, R. M.; Ellison, G. B. *J. Am. Chem. Soc.* **1985**, *107*, 109.
(30) DePuy, C. H.; Bierbaum, V. M. Schmitt, R. J.; Shapiro, R. H. *J. Am. Chem. Soc.* **1978**, *100*, 2920.
(31) Ingeman, S.; Kleingeld, J. C.; Nibbering, N. M. M. In *Ionic Processes in the Gas Phase*; Ferreira, M. A. A., Ed.; D. Reidel: Dordrecht, Holland, 1984.

Table V. Reactions of Nitrile Anions with $Fe(CO)_5$ at 0.4 torr

anion (R^-)	PA[a]	k^{11}[b]	eff	primary product ions (%)
$(CH_3)_2CCN^-$	373.8	1.2	0.69	$(CO)_4FeC(O)R^-$ (69) $(CO)_4FeR^-$ (23) $(CO)_4FeH^-$ (3) $(CO)_4FeCHO^-$ (5)
CH_3CHCN^-	373.7	1.2	0.64	$(CO)_4FeC(O)R^-$ (78) $(CO)_4FeR^-$ (20) $(CO)_3FeR^-$ (2)
CH_2CN^-	372.1	1.2	0.56	$(CO)_4FeC(O)R^-$ (82) $(CO)_4FeR^-$ (15) $(CO)_3FeR^-$ (3)

[a] Proton affinity in units of kcal mol^{-1}, ref 19. [b] In units of 10^{-9} cm^3 $molecule^{-1}$ s^{-1}.

products are observed, and neither the rate nor the branching ratio for the reaction changes with limited pressure variation (0.3 – 0.8 torr). Methyl carbonate reacts to give a single product corresponding to methoxide transfer (eq 6).

$$CH_3OCO_2^- + Fe(CO)_5 \rightarrow (CO)_4FeCO_2CH_3^- + CO_2 \quad (6)$$

Carbanions. A diverse set of carbanions covering a nearly 40 kcal mol^{-1} range in basicity have been reacted with $Fe(CO)_5$, including allylic, vinylic, benzylic, and acetylenic species. Table IV summarizes the measured kinetic data and product distributions at 0.4 torr. In addition to reactions as in eq 2, dissociative electron-transfer and hydride-transfer reactions are also observed in many cases. For example, both the allyl anion and the cyclohexadienyl anion produce $Fe(CO)_4^-$ as the major product ion (eq 7). While we do not detect neutral products in our exper-

$$CH_2CHCH_2^- + Fe(CO)_5 \rightarrow Fe(CO)_4^- + (C_3H_5 + CO) \quad (7)$$

iments, the assignment shown is reasonably secure since eq 7 is 5.6 kcal mol^{-1} exothermic as written, and the only other mechanistically feasible alternative, $CH_2{=}CHCH_2CO$, is thermodynamically unstable with respect to decarbonylation.[32] Applying similar reasoning and constraints to the appearance of $Fe(CO)_4^-$ from cyclohexadienyl anion provides an estimate of an upper limit for the electron affinity of c-C_6H_7 of 16.2 kcal mol^{-1}.[32] Addition of allyl anion to $Fe(CO)_5$ is also accompanied by expulsion of a single CO ligand. The highly basic phenide ion reacts with expulsion of up to two CO ligands, while the benzyl anion gives mainly addition along with smaller amounts of tetra- and tricarbonyl ion products. The carbanion derived from ethylbenzene causes loss of one CO, and traces of hydride transfer are also observed.[25] Acetylide ion behaves in a manner similar to benzyl in inducing losses of zero, one, and two CO ligands. Accurate determination of the branching ratio for this reaction could not be achieved due to the ubiquitous presence of $HC_2(H_2O)^-$ cluster ions in the system. All of the tricarbonyl primary products undergo further reaction with $Fe(CO)_5$ to yield dinuclear cluster complexes $RFe_2(CO)_n^-$ (n = 6–8). As with hydride, pressure-dependent branching ratios were encountered with certain of the carbanion reactants, but discussion of this will be deferred to a later section.

Nitriles and Nitrocarbanions. The conjugate base anions of simple aliphatic nitriles exhibit reactivity quite similar to the hydrocarbon ions except for the absence of electron-transfer reactions owing to their larger binding energies (Table V). Acetonitrile and propionitrile anions give mainly direct addition to $Fe(CO)_5$, with lesser amounts of single and double CO loss also observed. As with the enolates, the ambident nature of nitrile anions makes adduct–ion structural assignment ambiguous. Hydride transfer occurs with isobutyronitrile anion as described previously.[25] Pressure-dependent product distributions from 0.3 to 0.8 torr are evident for acetonitrile and propionitrile anions but not for the isobutyronitrile anion (vide infra). The prototype nitrocarbanion, $CH_2NO_2^-$ (derived by proton abstraction from CH_3NO_2) reacts rapidly (k = 1.4 × 10^{-9} cm^3 s^{-1}) to produce exclusively $Fe(CO)_4^-$, presumably by a dissociative electron-transfer reaction similar to eq 7. The low electron binding energy of $CH_2NO_2^-$ (EA = 11.5 kcal/mol)[33] can accommodate this mechanism, although others are also conceivable.

Azide. Azide ion is a familiar nucleophile from condensed-phase studies which undergoes an interesting set of reactions with $Fe(CO)_5$ in the gas phase. The ion is initially produced from the fast bimolecular reaction between NH_2^- and N_2O[24] (eq 8). The

$$NH_2^- + N_2O \rightarrow N_3^- + H_2O \quad (8)$$

ensuing reaction with $Fe(CO)_5$ (k = 8.6 × 10^{-10} cm^3 s^{-1}, eff = 0.41) produces two primary products at m/z 154 and m/z 182 in roughly equal amounts (eq 9). Two isobaric constitutions exist

$$N_3^- + Fe(CO)_5 \xrightarrow{a} Fe(CO)_2NCO^- + N_2 + 2CO \quad \text{or} \quad Fe(CO)_2N_3^- + 3CO \quad m/z\ 154$$

$$N_3^- + Fe(CO)_5 \xrightarrow{b} Fe(CO)_3NCO^- + N_2 + CO \quad \text{or} \quad Fe(CO)_3N_3^- + 2CO \quad m/z\ 182 \quad (9)$$

for each nominal mass which are not able to distinguish confidently from the observed isotopic abundances. Explusion of N_2 with formation of cyanate products is the precedented outcome in solution for group 6 hexacarbonyls,[34] and considering the reactivity observed for other anions, the loss of three CO ligands as shown in eq 9a seems unlikely. Interestingly, the more highly unsaturated primary product at m/z 154 undergoes secondary condensation reactions with $Fe(CO)_5$ to yield a dinuclear complex from which a single CO is lost (m/z 322).

Halide Ions. The halide ions F^-, Cl^-, Br^-, and I^- exhibit pronounced reactivity differences. For example, fluoride ion reacts rapidly with $Fe(CO)_5$ (k = 3.1 × 10^{-9} cm^3 s^{-1}; eff = 1.1) to produce all three addition/condensation products, $Fe(CO)_nX^n$, in an observed ratio at 0.4 torr of 92:2:6 for n = 3–5, respectively. A slight variation in this ratio occurs when the helium pressure is increased to 0.8 torr (85:2:13). In contrast, chloride ion reacts quite slowly (k = 3.1 × 10^{-11} cm^3 s^{-1}; eff = 0.014) and yields only the corresponding adduct. Br^- and I^- appear to be unreactive with $Fe(CO)_5$ under our conditions, although trace amounts of a Br^- adduct are detectable in the mass spectrum.

Comparison with Condensed-Phase Reactions. There are a large number of reports in the literature concerning condensed-phase nucleophilic reactions of $Fe(CO)_5$ with which the present results may be compared. A concise review of this chemistry is given by Collman.[5b] Nucleophilic addition reactions involving $Fe(CO)_5$ in solution generally give rise to the corresponding tetracarbonyl–acyl complexes, $(CO)_4FeC(O)X^-$, which are often directly characterized and occasionally isolable.[5,35-37] Certain nucleophiles may cause subsequent fragmentation and/or substitution in the acyl complex, depending upon the specific solvent and conditions employed. For example, $Fe(CO)_5$ readily reacts in aqueous alkaline solution to yield $HFe(CO)_4^-$ and CO_2; presumably through the intermediacy of a hydroxycarbonyl complex, $(CO)_4FeCO_2H^-$, which is unstable in aqueous solution.[13,20,38] This particular system has served as a model for water-gas shift catalysis in homogeneous solution.[12,39] With alkoxide ion nucleophiles in

(32) $EA(C_3H_5)$ = 8.35 ± 0.46 kcal mol^{-1}, $\Delta H_f[C_3H_5(g)]$ = 39.3 ± 0.8 kcal mol^{-1}: Oakes, J. M.; Ellison, G. B. *J. Am. Chem. Soc.* **1984**, *106*, 7734. $EA(Fe(CO)_4)$ = 55.3 ± 7.0 kcal mol^{-1}: Engelking, P. C.; Lineberger, W. C. *J. Am. Chem. Soc.* **1979**, *101*, 5569. $D[(CO)_4Fe{-}CO]$ = 41.5 ± 2 kcal mol^{-1}: Lewis, K. E.; Golden, D. M.; Smith, G. P. *J. Am. Chem. Soc.* **1984**, *106*, 3905. $\Delta H_f[CH_2{=}CHCH_2CO(g)]$ = 16 kcal mol^{-1}, estimated, cf.: Benson, S. W. *Thermochemical Kinetics*, 2nd Ed., Wiley: New York, 1976. $\Delta H_f[Fe(CO)_5(g)]$ = −173.0 ± 1.5 kcal mol^{-1}, $\Delta H_f[CO(g)]$ = −26.4 kcal mol^{-1}: Pedley, J. B.; Rylance, J. Sussex NPL Computer Analyzed Thermochemical Data, University Sussex, UK, 1977. Entropy contributions are incorporated in these estimations as given by simple statistical formulas.

(33) Tsuda, S.; Yokohata, A.; Kawai, M. *Bull. Chem. Soc. Jpn.* **1969**, *42*, 1515.

(34) Warner, H.; Beck, W.; Engelmann, H. *Inorg. Chem. Acta* **1969**, *3*, 331.

(35) (a) Nakamura, S.; Dedieu, A. *Theor. Chim. Acta* **1982**, *61*, 587. (b) Dedieu, A.; Nakamura, S. *Nouv. J. Chim.* **1984**, *8*, 317.

(36) Elzinga, J.; Hogeveen, H. *J. Chem. Soc., Chem. Commun.* **1977**, 705.

(37) Darensbourg, M. Y.; Condor, H. L.; Darensbourg, D. J. Hasday, C. *J. Am. Chem. Soc.* **1973**, *95*, 5919.

(38) Pearson, R. G.; Mauermann, H. *J. Am. Chem. Soc.* **1982**, *104*, 500.

Table VI. Summary of Reaction Products Resulting from Loss of CO Ligands Accompanying Nucleophilic Addition to $Fe(CO)_5$ at 0.4 torr

anion	PA[a]	eff	primary CO expulsion products $(CO)_3FeX^-$	$(CO)_4FeX^-$	$(CO)_4FeC(O)X^-$
NH_2^-	403.6	0.65	×		
H^-	400.4	0.40	×	×	
$C_6H_5^-$	398.8	0.85	×	×	
$CH_2{=}CH\text{-}CH_2^-$	391.3	0.52		×	×
OH^-	390.7	0.69	×		
CH_3O^-	381.4	0.76	×		
$PhCH_2^-$	379.2	0.83	×	×	×
$PhCHCH_3^-$	378.3	0.74		×	×
EtO^-	376.1	0.69	×		
HC_2^-	375.4	0.96	×	×	×
$(CH_3)_2CCN^-$	373.8	0.67	×	×	×
CH_3CHCN^-	373.7	0.61	×	×	×
$t\text{-}BuO^-$	373.3	0.95	×		
$MeOCH_2CH_2O^-$	372.5	1.1	×		
CH_2CN^-	372.1	0.57	×	×	×
F^-	371.3	1.1	×	×	×
$EtC(CH_3)_2O^-$	371.9	0.63	×		×
$nBuCH(CH_3)O^-$	371	0.93			×
$c\text{-}C_6H_7^-$	370	0.67			×
$CH_3COCH_2^-$	368.8	0.68			×
$CH_3COCHCH_3^-$	367.3	0.61			×
$CF_3CH_2O^-$	364.4	0.86	×		
EtS^-	359.0	0.66			×
HS^-	353.5	0.34			×
$CH_3CO_2^-$	348.5	0.08			×
HCO_2^-	345.2	0.08			×
N_3^-	344.6[b]	0.41		(see text)	
Cl^-	333.4	0.014			×
Br^-	323.6				
I^-	314.3				

[a] Proton affinity in units of kcal mol^{-1}, ref 19. [b] Pellerite, M. J.; Jackson, R. L.; Brauman, J. I. *J. Phys. Chem.* **1981**, *85*, 1624.

anhydrous solutions, the corresponding alkoxycarbonyls are produced exclusively.[5,13] A wide variety of carbanion analogues such as organolithium reagents and Grignard reagents react with $Fe(CO)_5$ in organic solvents.[8,9,40,41] The resulting acyl ion complexes are commonly trapped with alkylating agents to yield the well-known Fischer carbenes $(CO)_4Fe{=}C(OR)R'$.[5,8] Hydride donor reagents such as alkylborohydrides or alkoxyborohydrides produce a kinetically stable formyl complex, $(CO)_4FeCHO^-$, which may subsequently convert to the hydride $(CO)_4FeH^-$ at elevated temperatures.[7,25,42,43] Lithium dialkyl amides and a variety of neutral primary and secondary amines react with $Fe(CO)_5$ to yield the corresponding carbamoyl derivatives.[44] Finally, the strongly nucleophilic azide ion has been found to react readily with metal carbonyls to produce cyanate complexes by decomposition of the initially formed metalloazide $(CO)_nMC(O)N_3^-$ in a manner reminiscent of the Curtius reaction.[34]

Discussion

General Trends and Mechanism. We will initially focus discussion on the general mechanism for the reactions illustrated in eq 2 and the factors influencing the extent of CO expulsion from the adduct complexes. Table VI provides a summary overview of the reactivity observed for each of the anions described in the preceding sections. The negative ions are listed in order of decreasing proton affinity (PA)[19] with the observed extent of CO loss from reaction with $Fe(CO)_5$ indicated in the last three columns. The qualitative correlation between anion basicity and

Scheme I

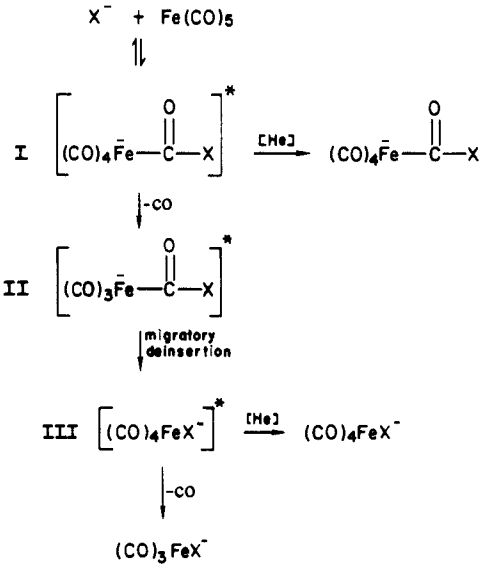

reactivity first noted by Beauchamp and Foster[16] is immediately evident in the table. In general, under flowing afterglow conditions the more strongly basic anions induce losses of one and/or two CO ligands from the adducts, while the weaker bases, that is, those anions with proton affinities less than ca. 370 kcal mol^{-1}, yield only the direct addition products. We recently described measurements of a series of negative ion binding energies of $Fe(CO)_5$, $D[(CO)_4FeCO\text{-}X^-]$, and illustrated how these data formed a linear correlation with the proton affinities of the negative ions.[28] That is, the relative energies of anion attachment to either a proton or an iron-bound carbonyl ligand are evidently proportional. Therefore, it is not surprising that the extent of CO loss accompanying covalent attachment of a negative ion to $Fe(CO)_5$ in the gas phase should correlate with the thermodynamic basicity and, thus, the $Fe(CO)_5$ binding energy of the anion. That is, the greater the binding energy of the anion, the greater the excess internal energy in the adduct which drives CO expulsion. However, closer inspection of the data in Table VI exposes some significant and mechanically revealing deviations from this qualitative trend. For instance, while OH^- and the allyl anion possess nearly identical proton affinities,[19] the smaller, heteroatomic OH^- induces the maximal loss of two CO ligands, whereas the carbanion causes loss of only one CO and produces a significant amount of adduct. This type of discrepancy is also evident for CH_3O^- and the two benzylic ions which possess nearly identical basicities but cause differing amounts of CO loss. Trifluoroethoxide ion, $CF_3CH_2O^-$, clearly stands out in Table VI in causing expulsion of two CO ligands while even stronger bases in its immediate vicinity, including the large alkoxide $n\text{-}BuCH(CH_3)O^-$, form only adducts.

We can account for the trends illustrated in Table VI with the stepwise mechanism for nucleophilic condensation reactions of $Fe(CO)_5$ shown in Scheme I. Addition of an anion reactant at carbon[35] initially gives rise to an iron tetracarbonyl–acyl complex I, which possesses an amount of excess internal energy equal to the covalent bond energy, $D[(CO)_4FeCO\text{-}X^-]$. In our previous study[28] we showed for many of the anions listed in Table V that this energy varies over a range of roughly 14–60 kcal mol^{-1}. If the energy is sufficiently large, then loss of a CO ligand may occur in competition with collisional stabilization of I by the helium buffer gas. Dissociation of a CO from iron produces a coordinatively unsaturated (16-electron) tricarbonyl–acyl ion II, which, if formed at all as a discrete intermediate, would be expected[45]

(39) Thompson, W. J.; Laine, R. M. *ACS Symp. Ser.* **1981**, *No. 152*, 133.
(40) Drew, D.; Darensbourg, M. Y.; Darensbourg, D. J. *J. Organomet. Chem.* **1975**, *85*, 73.
(41) Alper, H.; Fabre, J. *Organometallics* **1982**, *1*, 1037.
(42) Casey, C. P.; Neumann, S. M. *J. Am. Chem. Soc.* **1976**, *98*, 5395.
(43) Winter, S. R.; Cornett, G. M.; Thompson, E. A. *J. Organomet. Chem.* **1977**, *133*, 339.
(44) (a) Doxsee, K. M.; Grubbs, R. H. *J. Am. Chem. Soc.* **1981**, *103*, 7697. (b) Edgell, W. F.; Yang, M. T.; Bulkin, G. J.; Bayer, R.; Koizumi, N. *J. Am. Chem. Soc.* **1965**, *87*, 3080. (c) Edgell, W. F.; Bulkin, B. J. *J. Am. Chem. Soc.* **1966**, *88*, 4839.

(45) Coordinatively unsaturated iron carbonyl acyls are usually unstable with respect to migratory deinsertion in noncoordinating solvents, c.f. ref 5 and: Wojcicki, A. *Adv. Organomet. Chem.* **1973**, *11*, 87. An alternative structure for product *III* as the 18-electron η^2-acyl complex is contraindicated by the fact that these complexes are completely inert towards gas-phase addition reactions with σ-donor ligands such as CO and PF_3.

to succumb to rapid migratory deinsertion of X, yielding the more stable 18-electron iron tetracarbonyl anion complex, III. This exothermic rearrangment results in the accrual of an even greater amount of excess internal energy in intermediate III relative to the total energy of the reactants. Loss of a second CO to form $(CO)_3FeX^-$ may follow, again in competition with deactivating collisions by helium. Two alternative mechanisms deserve comment at this point. While direct associative displacement of CO also could conceivably produce $(CO)_nFeX^-$, $n = 3$ or 4 ions, such a mechanism is inconsistent with the observed pressure-dependent product distributions that will be described later. Furthermore, sequential expulsion of two CO ligands from I to yield a 14-electron acyl intermediate, $(CO)_2FeC(O)X^-$, can be ruled out on energetic grounds since the sum of the first two iron–carbonyl bond energies in I will generally exceed the total excess energy available in the system (vide infra). An important feature of the proposed mechanism is that it requires that the $(CO_4)FeX^-$ product form exclusively by way of a termolecular channel from intermediate III; i.e., there is no direct (bimolecular) route from I (or II). That this should be so is by no means obvious, and we have adopted this view for the following reasons. In both the earlier ICR studies of Beauchamp and Foster[16] and our own subsequent examination of several negative ion reactions with $Fe(CO)_5$ in a Fourier-transform mass spectrometer ($P \approx 10^{-7}$ torr),[46] the $(CO)_4FeX^-$ product has been conspicuously absent—even with reactant anions such as $C_6H_5^-$ which yield significant precentages of $(CO)_4FeX^-$ at 0.5 torr in the flowing afterglow. That is, under conditions approximating the low-pressure limit, reaction either produces only $(CO)_3FeX^-$ or does not occur at all.[47] Thus, a pressure-independent pathway for formation of a stable and observable $(CO)_4FeX^-$ product is unlikely. Moreover, we shall show later that if a $[(CO)_4FeX^-]^*$ intermediate is ever formed by fragmentation and rearrangement from $[(CO)_4FeC(O)X^-]^*$, then it will necessarily possess sufficient internal energy to expel the second CO. Therefore, under low-pressure conditions, where collisional deactivation is slow, all such $[(CO)_4FeX^-]^*$ ions will fragment.

To summarize Scheme I, at least two or perhaps three different intermediates obtain in the course of a single anion/$Fe(CO)_5$ collision, which ultimately leads to attachment of the nucleophile to iron and loss of CO ligands in competition with collisional deactivation. Therefore, the physically meaningful factors that determine the outcome for a particular anion are not only the initial binding energy, $D[(CO)_4FeCO\text{-}X^-]$, but also the relative lifetimes of intermediates I–III toward fragmentation and collisional stabilization, as well as the overall exothermicity for formation of $(CO)_3FeX^-$. An increased lifetime for I–III would disfavor fragmentation and facilitate termolecular reactions, while an increasing exothermicity for the reaction would favor fragmentation. Several properties of the reactant anions may be identified as potential influences on the reaction thermochemistry and the lifetimes and internal energies of the intermediates: anion basicity, the size of the anion, and the type of heteroatom at the nucleophilic site. As shown previously, the basicity of the anion reactant linearly correlates with its binding energy to $Fe(CO)_5$ and, therefore, with the total amount of excess internal energy present in the acyl intermediate I. As the size of the reactant anion and, thus, its total number of vibrational and rotational degrees of freedom increase, the lifetime of the initial adduct I and the tetracarbonyl complex III will increase. That is, the larger anions can endow the excited intermediates with a greater number of internal modes for excess energy dispersal. This may prolong their lifetime since CO loss requires energy localization into specific dissociative modes. As a result, collisional stabilization becomes more likely. The size effect is most clearly illustrated in the results for the alkoxide ion series (Table II), where the amount of double CO loss generally decreases with increasing alkoxide size until

Scheme II

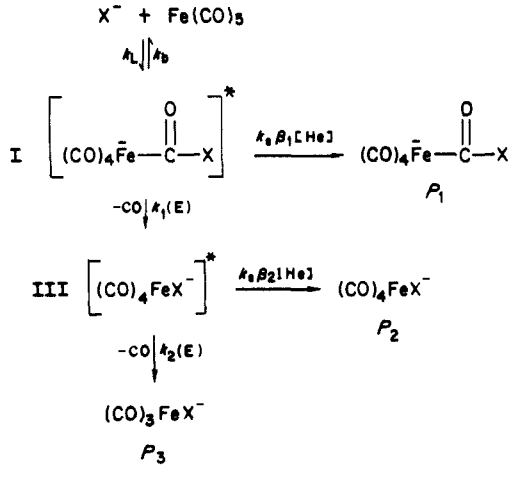

it is only barely discernible with $EtC(CH_3)_2O$ and disappears altogether with n-$BuCH(CH_3)O^-$. The slightly decreasing proton affinities down this series cannot be the cause, since loss of two CO ligands reappears for the smaller alkoxide $CF_3CH_2O^-$, despite its weaker basicity. The type of heteroatom at the nucleophilic site of the attacking anion can also exert a significant influence on the energetics for both the rearrangement step (II → III) and the ensuing CO loss from III since a new covalent bond to iron is formed at this site. In general, it is expected that lone-pair-bearing heteroatoms at the nucleophilic center such as O, N, or F will exert a (cis) CO-*labilizing* influence in $[(CO)_4FeX^-]^*$ intermediates that will be absent when X^- is a carbanion or hydride. This is due to repulsive d_π–p_π interactions between the lone-pair substituent and the coordinatively saturated (18-electron) metal center in $(CO)_4FeX^-$ which may reduce the Fe–CO bond energies, thereby facilitating CO loss in the activated ions.[48] An equivalent view is that lone-pair substituents can better stabilize the 16-electron dissociation products by π-donation, and, therefore, the iron–carbonyl bond energies are lessened.[49] The strong

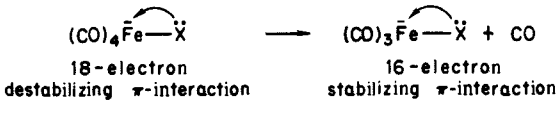

CO-labilizing effect of oxygen bases, halides, and other π-donor ligands has been extensively documented in condensed-phase ligand substitution reactions of metal carbonyls.[5,49] Such an effect satisfactorily accounts for the fact that all of the localized oxy anions (excluding n-$BuCH(CH_3)O^-$) produce *only* $(CO)_3FeOR^-$ products, while H^- and the carbanions of even greater basicities yield observable $(CO)_4FeR^-$ products. A similar reasoning may account for the low yield of $(CO)_4FeF^-$ observed from the F^- reaction.

Kinetic Model and Pressure Dependence. It is instructive to further consider the interplay of factors governing the extent of CO loss and the origins of the specific deviations from the general basicity/reactivity trend in terms of a kinetic model based on the mechanism shown in Scheme I. Scheme II represents a modified version of the mechanism in which we have ignored intermediate II for the sake of convenience since it is not essential to the model. The unimolecular rate constants for dissociation of the first and second CO ligands are $k_1(E)$ and $k_2(E)$, respectively, and are a function of the internal energy of the system, E. k_L and k_s are the Langevin rate coefficients[26] for the initial anion/$Fe(CO)_5$ collision and subsequent He collisions, respectively, while k_b represents the rate for back-dissociation of the initial adduct to reactants. The two collisional stabilization factors, β_1 and β_2, are

(46) Sallans, L.; Lane, K. R.; Freiser, B. S.; Squires, R. R., unpublished results.

(47) An exception to this is the formation of $Fe_2(CO)_8^-$ from the reaction between $Fe(CO)_5$ and the weakly basic $Fe(CO)_4^-$ anion, cf. Wronka, J.; Ridge, D. P. *J. Am. Chem. Soc.* **1984**, *106*, 67.

(48) For a recent example of the influence of this type of destabilizing interaction on ligand acidities, see: Buhro, W. E.; Georgiou, S.; Hutchinson, J. P.; Gladysz, J. A. *J. Am. Chem. Soc.* **1985**, *107*, 3346.

(49) (a) Lichtenberger, D. L.; Brown, T. L. *J. Am. Chem. Soc.* **1978**, *100*, 366. (b) Atwood, J. D.; Brown, T. L. *J. Am. Chem. Soc.* **1976**, *98*, 3155, 3160.

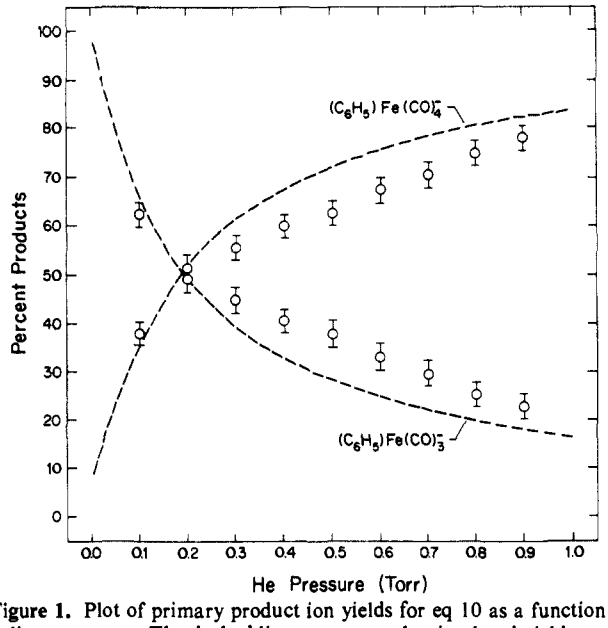

Figure 1. Plot of primary product ion yields for eq 10 as a function of helium pressure. The dashed line represents the simulated yield curves using the model depicted in Scheme II and $k_s = 5.4 \times 10^{-10}$ s^{-1}, $k_1/\beta_1 = 1.7 \times 10^{10}$ s^{-1}, and $k_2/\beta_2 = 3.4 \times 10^6$ s^{-1}.

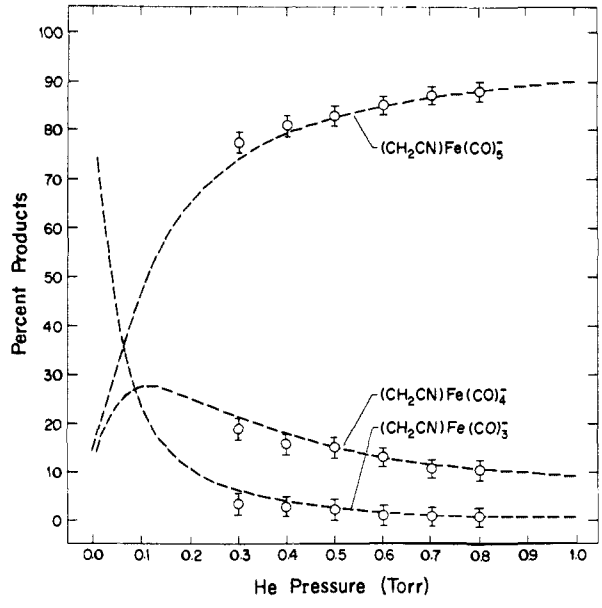

Figure 2. Plot of primary product ion yields vs. helium pressure for the reaction between $Fe(CO)_5$ and CH_2CN^-. The dashed line represents the simulated yield curves using the model depicted in Scheme II and $k_s = 5.4 \times 10^{-10}$ cm^3 s^{-1}, $k_1/\beta_1 = 1.9 \times 10^6$ s^{-1}, and $k_2/\beta_2 = 1.5 \times 10^6$ s^{-1}.

inversely proportional to the number of He collisions required to quench the first and second CO dissociations, respectively. In general, these factors will differ since the energies of the two fragmenting intermediates above threshold will differ. The relative product yields thus depend entirely upon the balance of dissociative rate coefficients k_1 and k_2, the changing internal energy of the intermediates relative to the total energy of the reactants, and the helium pressure. We can derive expressions for each of the product yields, $P_i/\sum P$, in terms of the microscopic rate coefficients in Scheme II where $P_1 = (CO)_4FeC(O)X^-$, $P_2 = (CO)_4FeX^-$, and $P_3 = (CO)_3FeX^-$

$$\frac{P_1}{\sum P} = \frac{k_s[He]}{(k_1/\beta_1) + k_s[He]}$$

$$\frac{P_2}{\sum P} = \frac{(k_1/\beta_1)k_s[He]}{(k_1/\beta_1 + k_s[He])(k_2/\beta_2 + k_s[He])}$$

$$\frac{P_3}{\sum P} = \frac{(k_1/\beta_1)(k_2/\beta_2)}{(k_1/\beta_1 + k_s[He])(k_2/\beta_2 + k_s[He])}$$

Each expression exhibits the proper limiting behavior; i.e., when [He] = 0 the yields of P_1 and P_2 are zero and $P_3/\sum P = 1.0$ (provided, of course, that it is energetically accessible). This was the case, for example, in the low-pressure ICR studies involving F^- and $CH_3CH_2O^-$. In the higher pressure limit, the yield of initial adduct P_1 approaches unity in an approximately logarithmic fashion while P_2 and P_3 drop off by roughly $P[He]^{-1}$ and $P[He]^{-2}$, respectively. It is clear from this model that, in general, for a reactant anion to form exclusively an iron tricarbonyl product (such as with OH^- and NH_2^-), both k_1/β_1 and k_2/β_2 must be greater than $k_s[He]$. Similarily, for anions to yield only adducts (such as the enolates), k_1/β_1 must be less than $k_s[He]$. The expected pressure dependence based on this model is nicely illustrated by the experimental data obtained for the hydrocarbon ions and nitrile ions alluded to earlier. Phenide ion provides an excellent case in point. Figure 1 shows a plot of the *primary* product ion yields for eq 10 as a function of the total pressure

$$C_6H_5^- + Fe(CO)_5 \rightarrow (CO)_4FeC_6H_5^- + CO$$
$$\rightarrow (CO)_3FeC_6H_5^- + 2CO \qquad (10)$$

in the flow reactor over the range 0.1–0.9 torr. Only the two fragmentation products shown above are produced over the entire pressure range, and no change in the measured rate of reaction is observed. The smooth increase in $(CO)_4FeC_6H_5^-$ at the expense of $(CO)_3FeC_6H_5^-$ with increasing pressure is typical behavior for a system in which fragmentation and stabilization channels compete from a single intermediate, in this case complex III. For example, Lias and co-workers recently reported pressure dependence of this kind of consecutive condensation reactions of hydrocarbon ions at high and low pressure.[50] In terms of the kinetic model in Scheme II, the complete absence of adduct $(CO)_4FeC(O)C_6H_5^-$ indicates that k_1 is substantially larger than $k_s\beta_1[He]$; therefore the first CO loss occurs rapidly following $C_6H_5^-$ addition. If we assume that the lower limit for detectable product in our instrument is 0.1% ($P_1/\sum P = 0.001$) and calculate $k_s = 5.4 \times 10^{-10}$ cm^3 s^{-1} from Langevin theory,[51] then it follows from the absence of P_1 at pressures up to 1.0 torr that $k_1/\beta_1 > 1.7 \times 10^{10}$ s^{-1}. That is, the initial adduct $[(CO)_4FeC(O)C_6H_5^-]^*$ cannot persist for more than ca. 60 ps prior to collisions with helium. Note that for $\beta_1 < 1.0$ (quite likely), longer total lifetimes would result. Similarly, the appearance of P_2 requires that k_2 have a value nearly equal to $k_s\beta_2[He]$. In fact, from the crossing point in the two experimental yield curves in Figure 1, where $P_2/\sum P = P_3/\sum P$, it can be shown that $k_2 = k_s\beta_2[He]$. Using $k_s = 5.4 \times 10^{-10}$ cm^3 s^{-1} and [He] = 0.2 torr = 6.4×10^{15} cm^{-3} from the observed crossing point leads to $k_2/\beta_2 = 3.5 \times 10^6$ s^{-1}. Therefore, the excited tetracarbonyl intermediate III must possess a lower limit to its dissociative lifetime of ca. 0.3 μs in order to account for the observed pressure dependence. Moreover, since β_2 (and β_1) are likely to be significantly less than 1.0, that is, since several He collisions are probably necessary to quench CO loss, the lifetime of $[(CO)_4FeC_6H_5^-]^*$ is probably somewhat greater than 0.3 μs. The calculated yield curves using $k_1/\beta_1 = 1.7 \times 10^{10}$ s^{-1} and $k_2/\beta_2 = 3.4 \times 10^6$ s^{-1} shown in Figure 1 are in good agreement with the experimental product distributions, although the calculated profiles exhibit somewhat greater curvature.

The nitrile anions and benzyl anion exhibit similar pressure-dependent behavior, as typified by that shown for CH_2CN^- in Figure 2. In this case an adduct complex is observed as the major product that appears to grow in at the expense of the single and double CO loss products at higher pressure. Here, k_1 and k_2 must be similar in magnitude to the dissociation quenching frequencies $k_s\beta_1[He]$ and $k_s\beta_2[He]$. From the yield equations given earlier,

(50) Buckley, T. J.; Sieck, L. W.; Metz, R.; Lias, S. G.; Liebman, J. F. *Int. J. Mass Spectrum. Ion Processes* **1985**, *65*, 181.

(51) An average reduced mass of 3.9 amu was used for these calculations, cf. ref 26.

Table VII. Limits on Dissociation Lifetimes for Negative Ion–$Fe(CO)_5$ Adducts Based on Pressure-Dependent Product Distributions

anion (A^-)	$(k_1/\beta_1)/(k_2/\beta_2)$[a]	$\tau[(CO)_4FeC(O)A^-]^*$, s	$\tau[(CO)_4FeA^-]^*$, s
H^-	>1200	$<6 \times 10^{-11}$ [b]	$>7 \times 10^{-8}$
$C_6H_5^-$	>4800	$<6 \times 10^{-11}$ [b]	$>3 \times 10^{-7}$
$C_6H_5CH_2^-$	0.14	$>9 \times 10^{-7}$	$>1 \times 10^{-7}$
CH_3CHCN^-	5.3	$>4 \times 10^{-7}$	$>2 \times 10^{-6}$
CH_2CN^-	1.3 ± 0.2	$>5 \times 10^{-7}$	$>6 \times 10^{-7}$
F^-	0.17	$>1 \times 10^{-8}$	$>2 \times 10^{-9}$

[a] Calculated from observed primary product yields and eq 11. [b] Assumes $\beta_1 = 1.0$; see text.

we can derive an expression for the ratio of fragmentation rates (eq 11). Using the experimental product yields for CH_2CN^-

$$(k_1/\beta_1)/(k_2/\beta_2) = P_2/P_1 + (P_2)^2/P_1P_3 \qquad (11)$$

observed over the range 0.3–0.7 torr gives an average value for $(k_1/\beta_1)/(k_2/\beta_2) = 1.3 \pm 0.2$. Moreover, since the yield of adduct, P_1, does not vary significantly over this range ($P_1/\sum P = 0.82 \pm 0.04$), we can estimate (k_1/β_1) as being equal to k_s[He](1.0 – 0.82)/0.82. Using $k_s = 5.4 \times 10^{-10}$ cm^3 s^{-1} and an average pressure [He] = 0.5 torr = 1.61×10^{16} cm^{-3} leads to $k_1/\beta_1 = 1.9 \times 10^6$ s^{-1}, and, from the above ratio, $k_2/\beta_2 = 1.5 \times 10^6$ s^{-1}. Therefore, the two consecutively formed intermediates are persisting a maximum of roughly 0.5 μs in the CH_2CN^- system—a factor of about 5 greater than the time between He collisions at 0.5 torr. The simulated product yield curves shown in Figure 2 using values of $k_1/\beta_1 = 1.9 \times 10^6$ s^{-1} and $k_2/\beta_2 = 1.5 \times 10^6$ s^{-1} are in good agreement with the experimental curves. A similar analysis for propionitrile, benzyl, hydride, and fluoride anions has been carried out and the data are summarized in Table VII. Hydride behaves like phenide ion, except that the $P_2 = P_3$ crossing point occurs at higher pressure (ca. 0.9 torr). All of the other anions listed in Table VII behave analogously to the CH_2CN^- system in that only slight pressure dependence is observed; therefore the systems were characterized in a similar manner. While pressure-dependent product distributions were observed for a few other reactant anions listed in Table VI, the occurrence of side reactions makes interpretation in terms of Scheme II difficult.

Energy Profile

It is possible to construct semiquantitative energy profiles for the negative ion–$Fe(CO)_5$ condensation reactions using thermodynamic data reported in our earlier study[28] along with the additional data derived below. Table VIII summarizes the relevant energetics for each of the negative ion reactants. The data pertain to eq 12 and 13, where $\Delta H(12)$ is given by the binding energy

$$X^- + Fe(CO)_5 \xrightarrow{\Delta H(12)} (CO)_4Fe(CO)X^- \qquad (12)$$

$$\Delta H(12) = -D[(CO)_4FeCO\text{–}X^-]$$

$$(CO)_4Fe(CO)X^- \xrightarrow{\Delta H(13)} (CO)_4FeX^- + CO \qquad (13)$$

$$\Delta H(13) = \Delta H_f[(CO)_4FeX^-(g)] + \Delta H_f[CO(g)] - \Delta H_f[(CO)_4FeC(O)X^-(g)]$$

of a negative ion to $Fe(CO)_5$ and, therefore, corresponds to the amount of excess internal energy present in the first reaction intermediate, I. $\Delta H(13)$ represents the enthalpy of CO deinsertion from the iron–acyl anion complexes and requires a knowledge of the thermochemistry for $(CO)_4FeX^-$ species. First of all, the negative ion binding energies of $Fe(CO)_5$ can be reasonably estimated with the basicity correlation equation which we described previously[28] (eq 14). Values for $\Delta H(12)$ computed in this way

$$D[(CO)_4FeCO\text{–}X^-] = 0.660PA(X^-) - 206 \text{ kcal mol}^{-1} \qquad (14)$$

for each of the reactant anions are collected in the third column of Table VIII. Comparison of these data with the CO loss distributions in Table VI indicates that the occurrence of fragmentation from the initial adduct generally coincides with anion binding energies greater than ca. 34 kcal mol^{-1}. That is, the excess energy in the excited acyl ion must exceed approximately 34 kcal mol^{-1} for the first CO loss to occur. Therefore, this quantity represents an estimate of the average CO dissociation activation

Table VIII. Thermochemical Data for Gas-Phase Reactions of Negative Ions with $Fe(CO)_5$[a]

anion, (X^-)	PA(X^-)	$D[(CO)_4FeCO\text{–}X^-]$[b]	$D[(CO)_4Fe\text{–}X^-]$[c]	$\Delta H(13)$[d]	$[\Delta H(12) + \Delta H(13)]$[e]
NH_2^-	403.6	60.4	110.3	−8.4	−68.8
H^-	400.4	58.2	107.7	−8.0	−66.2
$C_6H_5^-$	398.8	57.2	106.4	−7.7	−64.9
$CH_2CHCH_2^-$	391.3	52.4	100.6	−6.7	−59.1
OH^-	390.7	51.9[g]	100.0	−6.6	−58.5
CH_3O^-	381.4	45.7	92.6	−5.4	−51.1
$C_6H_5CH_2^-$	379.2	44.4	91.0	−5.1	−49.5
$C_6H_5CHCH_3^-$	378.3	43.7	90.1	−4.9	−48.6
$CH_3CH_2O^-$	376.1	42.2	88.4	−4.7	−46.9
HC_2^-	375.4	41.8	87.8	−4.5	−46.3
$(CH_3)_2CCN^-$	373.8	40.7	86.5	−4.3	−45.0
CH_3CHCN^-	373.7	40.6	86.4	−4.3	−44.9
$(CH_3)_3CO^-$	373.7	40.6	86.4	−4.3	−44.9
$CH_3OCH_2CH_2O^-$	372.5	39.9	85.5	−4.2	−44.1
CH_2CN^-	372.1	39.6	85.2	−4.1	−43.7
$CH_3CH_2C(CH_3)_2O^-$	371.9	39.5	85.0	−4.1	−43.6
F^-	371.3	39.0	84.5	−4.0	−43.0
$CH_3(CH_2)_3CH(CH_3)O^-$	371	38.9	84.3	−4.0	−42.8
c-$C_6H_7^-$	370	38.2	83.5	−3.8	−42.0
$CH_3COCH_2^-$ (C)	368.8[f]	37.4	82.6	−3.7	−41.1
$CH_3COCHCH_3^-$ (C)	367.3[f]	36.4	81.3	−3.4	−39.8
$CF_3CH_2O^-$	364.4	34.5	79.1	−3.1	−38.6
$CH_3CH_2S^-$	359.0	30.9	74.8	−2.3	−33.2
$CH_3COCH_2^-$ (O)	354.9[f]	28.2	71.5	−1.8	−30.0
HS^-	353.5	27.3	70.4	−1.6	−28.9
$CH_3CO_2^-$	348.5	24.0	66.4	−0.9	−24.9
HCO_2^-	345.2	21.8	63.8	−0.4	−22.2
N_3^-	344	21.0	62.8	−0.3	−21.3
Cl^-	333.4	14.0	54.4	1.1	−12.9
Br^-	323.6	7.6	46.6	2.5	−5.0
I^-	314.3	1.4	39.2	3.7	2.3

[a] All data in kcal mol^{-1}. [b] Calculated with eq 14; see ref 28. [c] Calculated with eq 15. [d] CO deinsertion enthalpy for iron tetracarbonyl–acyl anion complexes. [e] Enthalpy of reaction producing $XFe(CO)_4^-$ + CO from free X^- and $Fe(CO)_5$. [f] (C) = C–H acidity of keto form, (O) = O–H acidity of enol form. [g] Experimentally determined lower limit is 53.3 kcal mol^{-1}, ref 28.

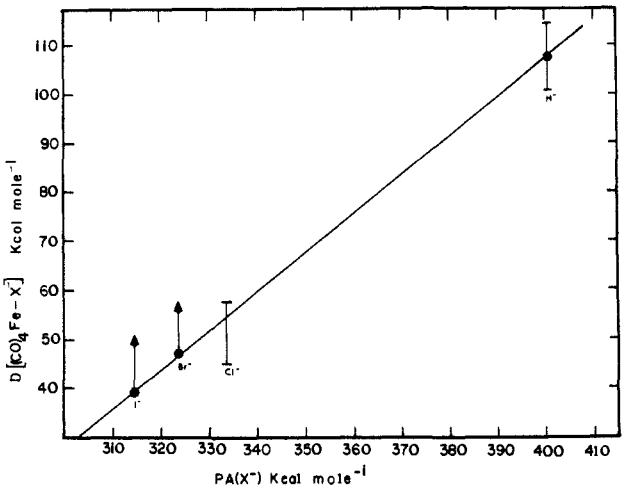

Figure 3. Plot of $Fe(CO)_4$ binding energy vs. proton affinity for negative ions: $D[(CO)_4Fe-H^-] = 107.4 \pm 6$ kcal mol^{-1} (ref 54 and 32); $D[(CO)_4Fe-Cl^-] = 79.2 \pm 6$ kcal mol^{-1}, $D[(CO)_4Fe-Br^-] > 69.2$ kcal mol^{-1}, $D[(CO)_4Fe-I^-] > 53.6$ kcal mol^{-1} (ref 53).

energy for $(CO)_4FeC(O)X^-$ ions. Furthermore, if we assume that CO loss from the iron–acyl produces a $(CO)_3FeC(O)X^-$ species lying close in energy to the transition state for the reaction (i.e., little or no reverse activation energy), then 34 kcal mol^{-1} represents an empirical estimate of the CO dissociation energy for iron–tetracarbonyl acyl anions. This is not unreasonable, considering the measured first Fe–CO bond energy (41.5 ± 2 kcal mol^{-1}) and the mean bond dissociation energy (28 kcal mol^{-1}) in $Fe(CO)_5$.[32] In considering the alternative reaction mechanism alluded to earlier wherein two CO ligands dissociate directly from the activated acyl ion complex I, we note that a rough estimate of the energy requirement for such a process as ca. $2 \times 34 = 68$ kcal mol^{-1} leads to an energy for $(CO)_2FeC(O)X^- + 2CO$ which is *greater* than that of the reactants in all cases listed in Table VIII. That is, the barrier for double CO loss without rearrangement of the metal ion products is likely to be prohibitive. It is also interesting to note in this context that the two ketone enolates did not induce any CO loss, even though their measured *carbon* basicities[19] suggest values of the initial $Fe(CO)_5$ binding energy that are greater than 34 kcal mol^{-1}. The *oxygen* basicity of each ion is reduced by the keto–enol energy difference for the neutrals (13 kcal mol^{-1} [52]) to such an extent that the estimated $Fe(CO)_5$ binding energies are less than 34 kcal mol^{-1}. These observations suggest that nucleophilic addition of ketone enolates to $Fe(CO)_5$ in the gas phase occurs through oxygen.[29]

We can obtain rough estimates of $\Delta H_f[(CO)_4FeX^-(g)]$ for use in evaluating eq 13 with an approach similar to that adopted for the acyl ions. A limited series of heterolytic bond dissociation energies for iron tetracarbonyl ions, $D[(CO)_4Fe-X^-]$, can be collected from the literature. Specifically, McDonald and coworkers[53] have determined limits for a few iron–halogen bond strengths from the observed gas-phase reactions of $Fe(CO)_4^-$, and a value for $D[(CO)_4Fe-H^-]$ can be derived from recent gas-phase acidity measurements for $(CO)_4FeH_2$.[54] These data define a rough linear correlation with the known proton affinities of each of the anions, as shown by the plot in Figure 3. The equation of the best straight line fitting the bounded and half-bounded data is given in eq 15. Therefore, within the limited accuracy of this

$$D[(CO)_4Fe-X^-] = 0.796PA(X^-) - 211 \text{ kcal mol}^{-1} \quad (15)$$

correlation (±5 kcal mol^{-1}), the binding energy of a negative ion to $Fe(CO)_4$ can be estimated from its proton affinity. Bond energies derived in this way are tabulated in the fourth column of Table VIII. Combining these data with $\Delta H_f[Fe(CO)_4(g)] = -105.6 \pm 2.5$ kcal mol^{-1} [32] and $\Delta H_f[X^-(g)]$ from gas-phase acidity

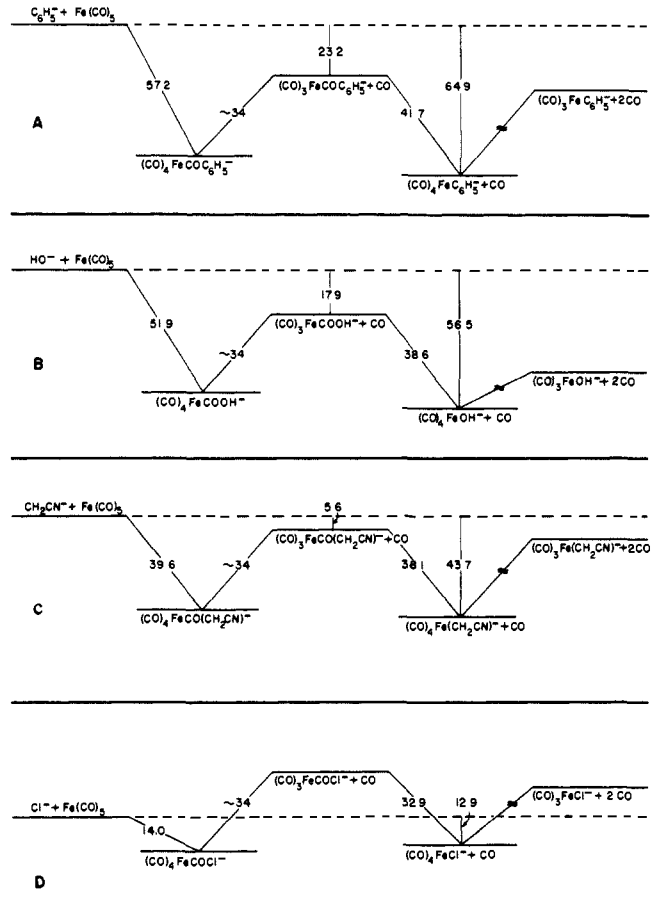

Figure 4. Semiquantitative energy profiles for gas-phase condensation reactions between negative ions and $Fe(CO)_5$. See text for derivation of parameters.

measurements for each of the anions[19] permits evaluation of $\Delta H_f[(CO)_4FeX^-(g)]$ as well as the corresponding values for the CO deinsertion enthalpies, $\Delta H(13)$. These are listed in the fifth column in Table VIII.[55] The sum $\Delta H(12) + \Delta H(13)$ gives the overall exothermicity for formation of $(CO)_4FeX^- + CO$ from X^- and $Fe(CO)_5$ and corresponds to a rough estimate of an *upper* limit for the amount of excess internal energy in the $[(CO)_4FeX^-]^*$ intermediates. These quantities are listed in the last column in the table. Consideration of their magnitudes underscores the importance of the heteroatom effect alluded to earlier. For example, the calculated maximum excess energy in the $[(CO)_4FeX^-]^*$ intermediates where X = H and C_6H_5 is 6–28 kcal mol^{-1} *greater* than that for intermediates where X = OR, yet the second CO ligand is always expelled from $[(CO)_4FeOR^-]^*$ complexes. Clearly, the actual magnitude of the second iron–carbonyl bond strength is a critical product-determining factor that may vary significantly with different anion reactants. Unfortunately, reliable data that might yield estimates of these quantities are not presently available. However, we can conclude that these bond energies must be somewhat less than the corresponding $\Delta H(13) + \Delta H(12)$ values listed in the upper part of Table VIII, since most all of the reactant anions producing a $(CO)_3FeX^-$ product did so rapidly and efficiently, and, therefore, the overall reactions must be substantially exothermic.

Energy profiles for the reactions of $Fe(CO)_5$ with $C_6H_5^-$, OH^-, CH_2CN^-, and Cl^- have been constructed from the data in Table VIII and are illustrated in Figure 4. Each profile, except for that of Cl^-, is characterized by a deep (covalent) energy well for the iron–acyl ion intermediate (I) with sufficient energy to overcome the approximately 34 kcal mol^{-1} barrier for loss of the first CO ligand. However, in the case of CH_2CN^- the top of the barrier is very near the limiting energy in the chemically activated system,

(52) Pollack, S. K.; Hehre, W. J. *J. Am. Chem. Soc.* **1977**, *99*, 4845.
(53) McDonald, R. N.; Schell, P. L.; McGhee, W. D. *Organometallics* **1984**, *3*, 182.
(54) Stevens, A. E.; Beauchamp, J. L., unpublished results.
(55) For an analysis of CO insertion energetics for manganese carbonyls, see: Simoes, J. A. M.; Beauchamp, J. L. *Chem. Rev.*, in press.

so passage over this barrier is relatively disfavored. Indeed, considering the crudeness of our approximations, it is even possible that the top of this barrier lies slightly above the energy of the initial reactants. As a result, these activated acyl ions persist longer, eventually partitioning between dissociation back to free reactants and dissociation of CO, with the latter process being slightly favored energetically and entropically. The key point here is that the relatively high CO dissociation barrier in this particular system makes collisional stabilization of the acyl complex favorable. That is, β_1 is likely to be near unity. The net result is a prepondence of adduct formation with only minor amounts of tri- and tetracarbonyl product being produced. The Cl^- profile represents the limiting case in which the barrier for CO loss is substantially greater than the initial activation energy in the acyl complex; thus, only back-dissociation or collisional stabilization can occur.

In contrast, in both the $C_6H_5^-$ and OH^- profiles the CO dissociation barriers are far below the energies of the reactants, so this mode of fragmentation proceeds rapidly from the energy-rich acyl ion complexes. That is, in these systems $k_1/\beta_1 \gg k_s$[He]. The migratory deinsertion step that follows releases on the average about 45 kcal mol^{-1} extra internal energy (maximum) into the iron tetracarbonyl complexes (III), resulting in energy levels for $(CO)_4FeX^-$ + CO that are lower than those of the corresponding acyl intermediates. This is true for most all of the ions listed in Table VIII. The final energy levels for the tricarbonyl complexes are not known. This level, along with the actual internal energy distributions of the $[(CO)_4FeX^-]^*$ complexes will determine the magnitude of k_2/β_2 and, thus, the relative yields of $(CO)_4FeX^-$ and $(CO)_3FeX^-$. From the complete absence of a $(CO)_4FeOH^-$ product in the OH^- reaction, we can infer that k_2/β_2 must be large and, accordingly, that D[$HOFe(CO)_3^-$–CO] is probably much less than the maximal 59.0 kcal mol^{-1} excess energy that is available to the tetracarbonyl intermediate. This is consistent with the heteroatom effect mentioned earlier. For the phenide system (Figure 4A), the high yield of $(CO)_4FeC_6H_5^-$ product despite an approximately 5 kcal mol^{-1} greater limit on the available excess energy in intermediate III suggests a somewhat smaller value of k_2/β_2. This implies that D[$C_6H_5Fe(CO)_3^-$–CO] is significantly greater than D[$HOFe(CO)_3^-$–CO]. Moreover, since the estimated energy profile for hydride is nearly identical with that for $C_6H_5^-$ and since H^- also produced a good yield of $(CO)_4FeH^-$, then it follows that nucleophile size is probably *not* a major influence in the appearance of tetracarbonyl product in these systems.

Finally, the data in Table VIII and the reaction profiles in Figure 4 provide some insight into the observed behavior of negative ion condensations with $Fe(CO)_5$ under low-pressure (ICR) conditions where reaction either yields only $(CO)_3FeX^-$ or does not occur at all.[47] It is evident in Table VIII that for all ions with $Fe(CO)_5$ binding energies exceeding the estimated 34 kcal mol^{-1} iron–acyl decarbonylation barrier the corresponding enthalpies for forming of $(CO)_4FeX^-$ (column 6) are all more negative than about −38 kcal $mol.^{-1}$ Therefore, each ion that is capable of inducing the first CO dissociation will yield a $[(CO)_4FeX^-]^*$ complex with nearly 38 kcal mol^{-1} excess internal energy. Since only tricarbonyl products were observed at low pressure, all such $[(CO)_4FeX^-]^*$ complexes must have fragmented and, therefore, the second iron carbonyl bond energies must be generally less than about 38 kcal mol^{-1}. Again, this is not unreasonable in view of the Fe–CO bond energies in $Fe(CO)_5$. The controlling factor for reactivity of $Fe(CO)_5$ under low-pressure conditions is therefore the initial energy of anion binding. Using eq 14, we can make the generalization that reactions at low pressure will produce only $(CO)_3FeX^-$ products with anions possessing proton affinities >364 kcal mol^{-1} and no products with anions of lower basicity.

Conclusion

The gas-phase reactions between negative ions and $Fe(CO)_5$ represent chemical systems that are rich in dynamic, mechanistic, and thermochemical information. A wide variety of anionic nucleophiles are found to react with $Fe(CO)_5$ at 0.1–0.9 torr total pressure by both addition and condensation reactions in which one or more CO ligands are displaced from the metal. Analysis of the observed reactivity patterns shows the following general trends: (1) most all anions react rapidly, with rates near the Langevin collision limit; (ii) the number of CO ligands displaced (zero, one, or two) generally correlates with the basicity of the nucleophile X^-, i.e., one and/or two CO losses result when $PA(X^-)$ > 364 kcal mol^{-1} and no CO loss occurs (simple adduct formation) when $PA(X^-)$ < 364 kcal mol^{-1}; (iii) localized anions with proton affinities >364 kcal mol^{-1} that possess lone-pair-bearing heteroatoms at the nucleophilic site yield exclusively iron tricarbonyl product ions by displacement of two CO ligands; (iv) as molecular complexity (size) and/or charge delocalization in the reactant anions increases, the extent of CO loss from the product ions decreases; (v) pressure-dependent product distributions are evident for certain of the reactions over the range 0.1–0.9 torr. A stepwise mechanism for anionic condensation reactions of $Fe(CO)_5$ is proposed to account for these trends wherein initial formation of an iron–acyl complex is followed by sequential dissociation of CO ligands in competition with collisional stabilization of the fragmenting intermediates. Loss of the first CO is accompanied in all cases by migratory deinsertion of the nucleophile to form an excited iron tetracarbonyl anion complex. Loss of the second CO may then occur in competition with deactivation by helium collisions. The apparent basicity/reactivity correlation reflects the energetics of the acyl-ion formation step; i.e., with greater anion basicity, the exothermicity for initial adduct formation and, therefore, the extent of CO loss from the products are greater. From the observed basicity/reactivity trends, general limits on the iron–carbonyl bond dissociation energies in $(CO)_4FeC(O)X^-$ and $(CO)_4FeX^-$ have been estimated to be <34 and <38 kcal mol^{-1}, respectively. The heteroatom effect is attributed to a specific weakening of the Fe–CO bond in $(CO)_4FeX^-$ when X is a π-donor ligand, and the size effect has its origins in the ability of large anion reactants to endow the nascent intermediates with longer lifetimes toward collisional stabilization. A detailed kinetic model is developed that quantitatively describes the competition between fragmentation and stabilization of the energy-rich intermediates. Limits on dissociative lifetimes for certain of the reaction complexes can be predicted from simulations of the observed pressure-dependent product distributions.

Reactions between anionic nucleophiles and $Fe(CO)_5$ in solution generally do not result in extensive CO loss from iron or formation of coordinatively unsaturated products, since any excess energy released during reaction is rapidly removed by the medium. Nevertheless, the present investigation of anionic condensation reactions of $Fe(CO)_5$ in the gas phase has provided useful information about the properties and dynamic behavior of several types of iron–carbonyl complexes—many of which have familiar analogues in condensed phases. The specific influence of solvation and counterions on nucleophilic reactions of metal carbonyls in solution is not well-defined at present, although recent progress has been made.[56] In order to begin an assessment of the thermochemical and dynamic role of solvent in these reactions, we are currently examining the reactions of *partially solvated* negative ions with $Fe(CO)_5$ in the gas phase. The results of this investigation will be presented in a future publication.

Acknowledgment. Part of this work was supported by the National Science Foundation (CHE-8502515). We are grateful to the donors of the Petroleum Research Fund, administered by the American Chemical Society, and to Research Corporation for their support in the construction of our instrument. K.R.L. thanks Procter and Gamble for a fellowship.

Registry No. $Fe(CO)_5$, 13463-40-6; NH_2^-, 17655-31-1; H^-, 12184-88-2; OH^-, 14280-30-9; CH_3O^-, 3315-60-4; $CH_3CH_2O^-$, 16331-64-9; $(CH_3)_3CO^-$, 16331-65-0; $CH_3OCH_2CH_2O^-$, 33175-38-1; CH_3CH_2C(C-

(56) (a) Kao, S. C.; Darensbourg, M. Y.; Schenk, W. *Organometallics* **1984**, *3*, 871. (b) Darsenbourg, D. J.; Baldwin, B. J.; Froelich, J. A. *J. Am. Chem. Soc.* **1980**, *102*, 4688. (c) Darensbourg, M. Y.; Darensbourg, D. J.; Barros, H. L. C. *Inorg. Chem.* **1978**, *17*, 297. (d) Darensbourg, D. J.; Ovalles, C. *J. Am. Chem. Soc.* **1984**, *106*, 3750.

$H_3)_2O^-$, 62002-46-4; $CH_3(CH_2)_3CH(CH_3)O^-$, 102494-15-5; $CF_3CH_2O^-$, 24265-37-0; HCO_2^-, 71-47-6; $CH_3CO_2^-$, 71-50-1; $CH_3OCO_2^-$, 616-38-6; $C_6H_5^-$, 2396-01-2; $CH_2{=}CHCH_2^-$, 1724-46-5; $C_6H_5CH_2^-$, 18860-15-6; $C_6H_5CHCH_3^-$, 13822-53-2; HC_2^-, 29075-95-4; c-$C_6H_7^-$, 102494-16-6; $(CH_3)_2CCN^-$, 102494-17-7; CH_3CHCN^-, 42117-12-4; CH_2CN^-, 21438-99-3; F^-, 16984-48-8; $CH_3COCH_2^-$, 24262-31-5; $CH_3COCHCH_3^-$, 64723-99-5; EtS^-, 20733-13-5; HS^-, 15035-72-0; N_3^-, 14343-69-2; Cl^-, 16887-00-6; Br^-, 24959-67-9; I^-, 20461-54-5.

Vibrational Spectra of $C_3H_3^+$, $C_3D_3^+$, $C_3H_2D^+$, and $C_3D_2H^+$ and Force Constants for This Ion System

Norman C. Craig,* Julianto Pranata, Sara Jamie Reinganum, Julian R. Sprague, and Philip S. Stevens

Contribution from the Department of Chemistry, Oberlin College, Oberlin, Ohio 44074.
Received February 5, 1986

Abstract: Infrared and Raman spectra of the four hydrogen–deuterium isotopomers of the cyclopropenyl cation, $C_3H_3^+$, $C_3D_3^+$, $C_3H_2D^+$, and $C_3D_2H^+$, have been recorded. A virtually complete assignment has been made of the spectroscopically active, in-plane fundamentals of the set of four ions. Assignments for the out-of-plane vibrational modes are fragmentary. For the $C_3H_3^+$ ion, the frequencies (cm^{-1}) are as follows: a_1' 3183, 1626; a_2' (1031); e' 3138, 1290, 927; a_2'' 758; e'' (990), where the values in parentheses are from normal coordinate calculations. A complete, general-valence force field of 12 constants has been fitted to the set of 31 observed frequencies. Force constants for CC stretching (7.890 mdyn $Å^{-1}$), CH stretching (5.284 mdyn $Å^{-1}$), and CH in-plane bending (0.599 mdyn Å rad^{-2}) are each larger than the corresponding force constants for benzene. The large force constant for CC stretching implies that the cyclopropenyl cation has exceptionally strong π-bonding.

Breslow and co-workers first prepared the unsubstituted cyclopropenyl cation in the late 1960s.[1] As part of the characterization of this simplest of aromatic species, they recorded infrared spectra of the $C_3H_3^+SbCl_6^-$, $C_3H_3^+AlCl_4^-$, and $C_3D_3^+SbCl_6^-$ salts and assigned the infrared-active fundamentals of the cations.[1b] To help define the bonds experimentally in this cation system, force constants for various bond motions are needed. Useful normal coordinate calculations for this purpose depend on having vibrational assignments from Raman spectra as well as from infrared spectra and on additional experimental data such as vibrational frequencies for several isotopic modifications. A previous, selective fitting of force constants of the cyclopropenyl cation was done for the fragmentary assignment of fundamentals.[2]

We now report an infrared and Raman investigation of the full set of hydrogen–deuterium isotopomers, $C_3H_3^+$, $C_3D_3^+$, $C_3H_2D^+$, and $C_3D_2H^+$. In a preliminary account we gave the results for the in-plane vibrational fundamentals of the first three ions and reported force constants for CC stretching, CH stretching, and CH bending coordinates that were larger than the corresponding values in benzene, the standard of aromaticity.[3] The unusually large CC stretching force constant for the cyclopropenyl cation had been anticipated by the ab initio calculation of Takada and Ohno.[4] The present report, which includes the results of normal coordinate calculations for the full set of four isotopomers, confirms the preliminary findings and adds results for the out-of-plane modes. In addition, these calculations define the complete set of 12 general-valence force constants for the cyclopropenyl cation. Such a complete determination of a force field from frequencies for hydrogen–deuterium isotopomers alone is an exceptional outcome for a hexatomic species.

The role of cyclopropenyl cations in solution-phase and solid-phase chemistry is well-known. Not so well recognized is the importance of the cyclopropenyl cation in non-sooting, fuel-rich flames.[5] Because of its atomic simplicity, yet prime position as an aromatic species, the cyclopropenyl cation is of considerable interest in theoretical chemistry.

The $C_3H_3^+$ and $C_3D_3^+$ ions were prepared by reaction of 3-chlorocyclopropene and 3-chlorocyclopropene-d_3, respectively, with Lewis acids, which included BF_3, SbF_5, and BCl_3. These two chlorocyclopropenes were made by reducing tetrachlorocyclopropene with tributyltin hydride and tributyltin deuteride, respectively.[1] To obtain the isotopically mixed species, $C_3H_2D^+$ and $C_3D_2H^+$, a two-step reduction sequence was applied to tetrachlorocyclopropene. For production of the first of these ions, tetrachlorocyclopropene was reduced with the hydride to an inseparable mixture of the isomers, 1,3-dichlorocyclopropene and 3,3-dichlorocyclopropene.[1c] This mixture was then reduced with the deuteride to a mixture of 3-chlorocyclopropene-*1*-d_1 and 3-chlorocyclopropene-*3*-d_1. Reaction of this mixture of isotopomers with a Lewis acid gave the single cation $C_3H_2D^+$. Exchanging the order of reduction of tetrachlorocyclopropene with the hydride and the deuteride led to $C_3D_2H^+$.

3-Fluorocyclopropene was also prepared and evaluated as a precursor of the cyclopropenyl cation.[6] However, this halocyclopropene was uncontrollably reactive with BF_3 in sulfur dioxide solution and thus useless for Raman spectroscopy. With difficulty the low-temperature, bilayer reaction technique was used with 3-fluorocyclopropene and BF_3 to prepare samples of the cation for infrared spectroscopy.

Experimental Section

Syntheses. The synthesis of 3-chlorocyclopropene (**1**) by reduction of tetrachlorocyclopropene with tri-*n*-butyltin hydride has been described.[1,6] Typically, about one-third of the crude product, the more volatile part consisting mostly of cyclopropene, acetylene, and hydrogen chloride, was removed by bulb-to-bulb distillation before resorting to preparative GC. In the GC separation[1c] at room temperature the elution time of **1** was 5 relative to that of the cyclopropene–acetylene mixture. The principal fractions that appeared between these two peaks were 1-butene, 1-chlorocyclopropene, and propargyl chloride, $CH_2ClC{\equiv}CH$.

3-Chlorocyclopropene-d_3 (**2**) was made by the same method as was used for the d_0 isotopomer except for substitution of tributyltin deuteride (Alfa Products, Morton Thiokol, Inc.) for the hydride. Principal IR

(1) (a) Breslow, R.; Groves, J. T.; Ryan, G. *J. Am. Chem. Soc.* **1967**, *89*, 5048. (b) Breslow, R.; Groves, J. T. *J. Am. Chem. Soc.* **1970**, *92*, 984–987. (c) Breslow, R.; Ryan, G.; Groves, J. T. *J. Am. Chem. Soc.* **1970**, *92*, 988–993.
(2) Yoshida, Z.-I.; Hirota, S.; Ogoshi, H. *Spectrochim. Acta* **1974**, *30A*, 1105–1114.
(3) Craig, N. C.; Pranata, J.; Sprague, J. R.; Stevens, P. S. *J. Am. Chem. Soc.* **1984**, *106*, 7637–7638.
(4) Takada, I.; Ohno, K. *Bull. Chem. Soc. Jpn.* **1979**, *52*, 334–338.
(5) Olson, D. B.; Calcote, H. F. *Symp. (Int.) Combust. [Proc.]* **1980** (Pub. 1981), *18*, 453–464.
(6) Craig, N. C.; Sloan, K. L.; Sprague, J. R.; Stevens, P. S. *J. Org. Chem.* **1984**, *49*, 3847–3848.

0002-7863/86/1508-4378$01.50/0